

# The web of human sexual contacts

Promiscuous individuals are the vulnerable nodes to target in safe-sex campaigns.

Unlike clearly defined 'real-world' networks<sup>1</sup>, social networks tend to be subjective to some extent<sup>2,3</sup> because the perception of what constitutes a social link may differ between individuals. One unambiguous type of connection, however, is sexual contact, and here we analyse the sexual behaviour of a random sample of individuals<sup>4</sup> to reveal the mathematical features of a sexual-contact network. We find that the cumulative distribution of the number of different sexual partners in one year decays as a scale-free power law that has a similar exponent for males and females. The scale-free nature of the web of human sexual contacts indicates that strategic safe-sex campaigns are likely to be the most efficient way to prevent the spread of sexually transmitted diseases.

Many real-world networks<sup>1</sup> typify the 'small-world' phenomenon<sup>5</sup>, so called because of the surprisingly small average path lengths between nodes<sup>6,7</sup> in the presence of a large degree of clustering<sup>3,6</sup> (Fig. 1). Small-world networks are classed as single-scale, broad-scale or scale-free, depending on their connectivity distribution,  $P(k)$ , where  $k$  is the number of links connected to a node<sup>8</sup>. Scale-free networks, which are characterized by a power-law decay of the cumulative distribution  $P(k) \approx k^{-\alpha}$ , may be formed as a result of preferential attachment of new links between highly connected nodes<sup>9,10</sup>.

We analysed the data gathered in a 1996 Swedish survey of sexual behaviour<sup>4</sup>. The survey involved a random sample of 4,781 Swedes (aged 18–74 years) and used structured personal interviews and question-

naires. The response rate was 59%, which corresponds to 2,810 respondents. Two independent analyses of non-response error revealed that elderly people, particularly women, are under-represented in the sample; apart from this skew, the sample is representative in all demographic dimensions.

Connections in the network of sexual contacts appear and disappear as sexual relations are initiated and terminated. To investigate the connectivity of this dynamic network, in which links may be short-lived, we first analysed the number,  $k$ , of sex partners over a relatively short time period — the 12 months before the survey. Figure 2a shows the cumulative distribution,  $P(k)$ , for female and male respondents. The data closely follow a straight line in a double-logarithmic plot, which is consistent with a power-law dependence. Males report a larger number of sexual partners than females<sup>11</sup>, but both show the same scaling properties.

These results contrast with the exponential or gaussian distributions — for which there is a well-defined scale — found for friendship networks<sup>8</sup>. Plausible explanations for the structure of the sexual-contact network described here include increased skill in acquiring new partners as the number of previous partners grows, varying degrees of attractiveness, and the motivation to have many new partners to sustain self-image. Our results are consistent with the preferential-attachment mechanism of scale-free networks: **evidently, in sexual-contact networks, as in other scale-free networks, 'the rich get richer'**<sup>9,10</sup>.

We next analysed the total number of



**Figure 1** It's a small world: social networks have small average path lengths between connections and show a large degree of clustering. Painting by Idahlia Stanley.

partners,  $k_{\text{tot}}$ , in the respondent's life up to the time of the survey. This value is not relevant to the instantaneous structure of the network, but may help to elucidate the mechanisms responsible for the distribution of number of partners. Figure 2b shows the cumulative distribution,  $P(k_{\text{tot}})$ : for  $k_{\text{tot}} > 20$ , the data follow a straight line in a double-logarithmic plot, which is consistent with a power-law dependence in the tails of the distribution.

Our most important finding is the scale-free nature of the connectivity of an objectively defined, non-professional social network. This result indicates that the concept of the 'core group' considered in epidemiological studies<sup>12</sup> must be arbitrary, because there is no well-defined threshold or boundary that separates the core group from other individuals (as there would be for a bimodal distribution).

Our results may have epidemiological implications, as epidemics arise and propagate much faster in scale-free networks than in single-scale networks<sup>6,13</sup>. Also, the measures adopted to contain or stop the propagation of diseases in a network need to be radically different for scale-free networks. Single-scale networks are not susceptible to attack at even the most connected nodes, whereas scale-free networks are resilient to random failure but are highly susceptible to destruction of the

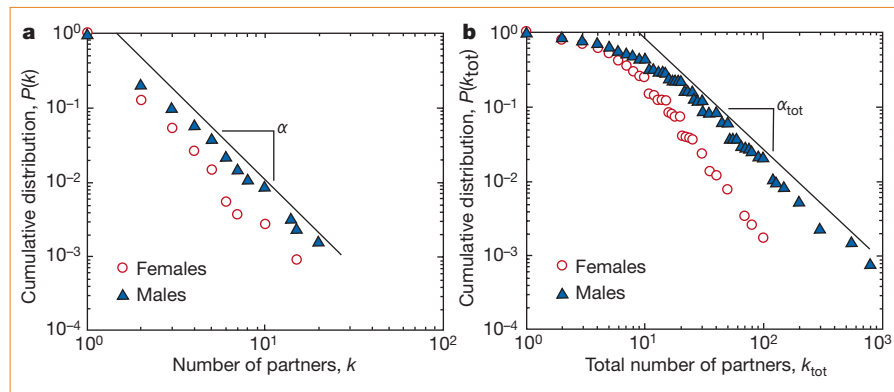


**Figure 2** Scale-free distribution of the number of sexual partners for females and males. **a**, Distribution of number of partners,  $k$ , in the previous 12 months. Note the larger average number of partners for male respondents: this difference may be due to 'measurement bias' — social expectations may lead males to inflate their reported number of sexual partners. Note that the distributions are both linear, indicating scale-free power-law behaviour. Moreover, the two curves are roughly parallel, indicating similar scaling exponents. For females,  $\alpha = 2.54 \pm 0.2$  in the range  $k > 4$ , and for males,  $\alpha = 2.31 \pm 0.2$  in the range  $k > 5$ . **b**, Distribution of the total number of partners  $k_{\text{tot}}$  over respondents' entire lifetimes. For females,  $\alpha_{\text{tot}} = 2.1 \pm 0.3$  in the range  $k_{\text{tot}} > 20$ , and for males,  $\alpha_{\text{tot}} = 1.6 \pm 0.3$  in the range  $20 < k_{\text{tot}} < 400$ . Estimates for females and males agree within statistical uncertainty.

best-connected nodes<sup>14</sup>. The possibility that the web of sexual contacts has a scale-free structure indicates that strategic targeting of safe-sex education campaigns to those individuals with a large number of partners may significantly reduce the propagation of sexually transmitted diseases.

Fredrik Liljeros\*, Christofer R. Edling\*, Luis A. Nunes Amaral†, H. Eugene Stanley†, Yvonne Åberg\*

\*Department of Sociology, Stockholm University, S-106 91 Stockholm, Sweden  
e-mail: liljeros@sociology.su.se

†Center for Polymer Studies and Department of Physics, Boston University, Boston, Massachusetts 02215, USA

1. Strogatz, S. H. *Nature* **410**, 268–276 (2001).
2. Kochen, M. (ed.) *The Small World* (Ablex, Norwood,

New Jersey, 1989).

3. Wasserman, S. & Faust, K. *Social Network Analysis* (Cambridge Univ. Press, Cambridge, 1994).
4. Lewin, B. (ed.) *Sex i Sverige. Om Sexuallivet i Sverige 1996* [Sex in Sweden. On the Sexual Life in Sweden 1996] (Nat Inst. Pub. Health, Stockholm, 1998).
5. Milgram, S. *Psychol. Today* **2**, 60–67 (1967).
6. Watts, D. J. & Strogatz, S. H. *Nature* **393**, 440–442 (1998).
7. Barthélemy, M. & Amaral, L. A. N. *Phys. Rev. Lett.* **82**, 3180–3183 (1999).
8. Amaral, L. A. N., Scala, A., Barthélemy, M. & Stanley, H. E. *Proc. Natl Acad. Sci. USA* **97**, 11149–11152 (2000).
9. Simon, H. A. *Biometrika* **42**, 425–440 (1955).
10. Barabási, A.-L. & Albert, R. *Science* **286**, 509–512 (1999).
11. Laumann, E. O., Gagnon, J. H., Michael, R. T. & Michaels, S. *The Social Organization of Sexuality* (Univ. Chicago Press, Chicago, 1994).
12. Hethcote, H. W. & Yorke, J. A. *Gonorrhea Transmission Dynamics and Control* (Springer, Berlin, 1984).
13. Pastor-Satorras, R. & Vespignani, A. *Phys. Rev. Lett.* **86**, 3200–3203 (2001).
14. Albert, R., Jeong, H. & Barabási, A.-L. *Nature* **406**, 378–382 (2000).

## Biomechanics

# Turning the key on *Drosophila* audition

The genetic dissection of *Drosophila* audition is advancing considerably<sup>1–4</sup>, but complementary studies are needed to unravel the chain of mechanosensory events that bring about hearing in the fly<sup>5</sup>. Here we investigate the delicate biomechanics of the fly's minute antennal hearing organs and show that they look and work like a lock and key. Rotating in response to sound, the antenna's distal segment mechanically activates the auditory receptors — thereby 'unlocking' the mechanism

of *Drosophila* audition.

In *Drosophila melanogaster*, the antennae mediate the detection of conspecific 'love songs'<sup>5,6</sup>. Anatomically, each antenna is an asymmetric structure consisting of three segments and a feather-like arista<sup>3</sup> (Fig. 1a). Laser vibrometric analysis of sound-induced vibrations<sup>7</sup> reveals that the arista and the club-shaped third segment together constitute a mechanical entity — the sound receiver. Both antennal parts oscillate sympathetically in response to acoustic stimulation, consistently exhibiting a moderately damped resonance at  $426 \pm 16$  Hz (quality factor,  $Q = 1.2 \pm 0.1$ ; 8 flies; Fig. 1b).

Mechanical measurements at different locations (Fig. 1b) show that the entire

arista oscillates as a stiff rod, with its vibration velocity continuously decreasing from tip to base. Remarkably, this oscillation is accompanied by rotation of the third segment. The 180° phase shift between the mechanical responses of opposite edges (Fig. 1b) unambiguously shows that they move in opposite directions and that this segment rotates about its longitudinal axis. This rotation is a direct consequence of the radial orientation of the arista, which breaks mechanical symmetry. Physically, the arista introduces a moment arm, increases the effective surface area, and thus determines the twisting force (torque) exerted by sound.

When stimulated acoustically, the third segment rotates like the bow of a key (Fig. 1c). Moreover, the proximal part of this segment presents a stalk that fits into a pit in the second segment, like a key in its lock. Extending along the rotational axis, this stalk transmits the rotation 'downstream', like a key's stem (Fig. 1a, c). Before connecting to the second segment, the stalk bends, forming a hook. This hook then oscillates like a key's bit (Fig. 1a, c). This vibration will maximally stretch and compress the auditory receptors which, notably, are attached perpendicularly to both sides of the hook.

Unlike other animals, *Drosophila* makes use of sound-induced rotation to channel acoustic energy to its auditory receptor neurons — it has 'rotational ears'. This unconventional mechanism relies on a simple trick: the hook balances the asymmetry introduced by the arista, thereby guaranteeing a receptor activation that compares to that in other insect auditory systems<sup>8</sup>. The third segment of the *Drosophila* antenna is also the primary organ of olfaction and carries hundreds of olfactory sensilla<sup>9</sup>. As hearing relies on rotation, the two sensory modalities can co-exist without compromising their respective functions. Such an evolutionary solution is elegant; flies did not turn their nose into an ear, they turn their nose to hear.

Martin C. Göpfert, Daniel Robert

Institute of Zoology, University of Zurich, Winterthurerstrasse 190, CH-8057 Zurich, Switzerland

e-mail: mgöpfert@zool.unizh.ch

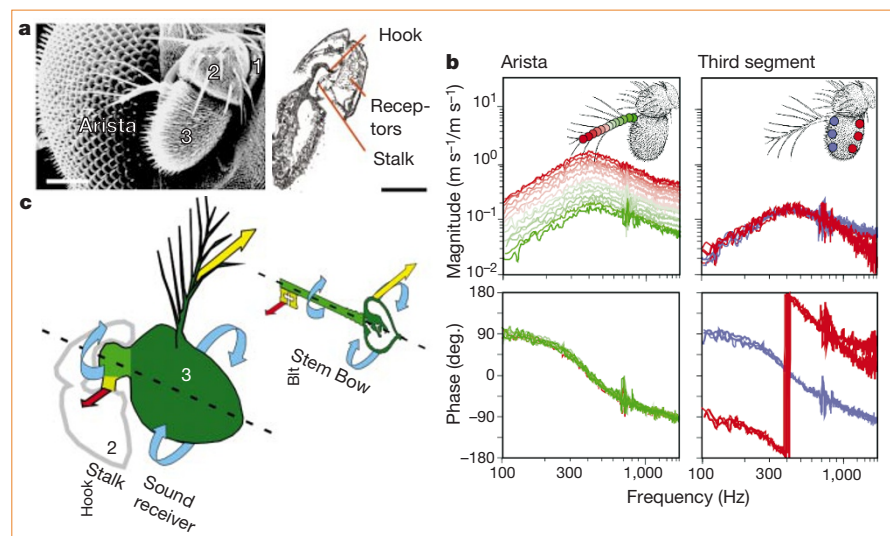


**Figure 1** Anatomy, mechanical response and operational mode of *Drosophila* antennal hearing organs. **a**, Anatomy. Left panel, scanning electron micrograph showing the three antennal segments (numbered) and the arista; right panel, longitudinal section through segments 2 and 3. Scale bars, 100  $\mu$ m. **b**, Mechanical response to acoustic random-noise stimulation. The arista and the third segment exhibit identical resonance characteristics and rotate about the longitudinal axis of the latter. Frequency spectra show the magnitude and phase of the vibration velocity (measured by microscanning laser Doppler vibrometry<sup>7</sup>) normalized to the particle velocity in the sound field (measured by a particle-velocity microphone at the antenna's position<sup>7</sup>). A response magnitude of unity indicates equal vibration velocity and particle velocity, and a phase of +90° means that the vibration velocity leads the particle velocity by one-quarter of an oscillation cycle. The acoustic stimulus (mean particle velocity  $\pm 0.04$  mm s<sup>-1</sup>) induced maximal displacements of  $\pm 20$  nm and rotation of  $\pm 0.003^\circ$ . Insets, measurement sites and colour convention (drawing by P. Bryant<sup>19</sup>). **c**, Operational mode, showing analogy between antennal mechanics and a rotating key. Yellow arrows, input force; blue arrows, rotation; red arrows, output force.

1. Kernan, M., Cowan, D. & Zuker C. *Neuron* **12**, 1195–1206 (1994).
2. Eberl, D. F., Duyk, G. M. & Perrimon, N. *Proc. Natl Acad. Sci. USA* **94**, 14837–14842 (1997).
3. Eberl, D. F., Hardy, R. W. & Kernan, M. J. *J. Neurosci.* **20**, 5981–5988 (2000).
4. Walker, R., Willingham, A. & Zuker C. *Science* **287**, 2229–2234 (2000).
5. Bennet-Clark, H. C. *Nature* **234**, 255–259 (1971).
6. Hall, J. C. *Science* **264**, 1702–1714 (1994).
7. Göpfert, M. C. & Robert, D. *Proc. R. Soc. Lond. B* **267**, 453–457 (2000).
8. Yager, D. D. *Microsc. Res. Tech.* **47**, 380–400 (1999).
9. Carlson, J. R. *Trends Genet.* **12**, 175–180 (1996).
10. FlyBase consortium (<http://flybase.bio.indiana.edu>) *Nucleic Acids Res.* **27**, 85–88 (1999).